We are IntechOpen,
the world's leading publisher of
Open Access books
Built by scientists, for scientists

5,400
Open access books available

133,000
International authors and editors

165M
Downloads

Our authors are among the

154
Countries delivered to

TOP 1%
most cited scientists

12.2%
Contributors from top 500 universities

CLARIVATE ANALYTICS
BOOK CITATION INDEX
INDEXED

WEB OF SCIENCE™

Selection of our books indexed in the Book Citation Index
in Web of Science™ Core Collection (BKCI)

Interested in publishing with us?
Contact book.department@intechopen.com

Experiences in Recognizing Free-Shaped Objects from Partial Views by Using Weighted Cone Curvatures

Carlos Cerrada[1], Santiago Salamanca[2], Antonio Adan[3],
Jose Antonio Cerrada[1] and Miguel Adan[3]
[1]Universidad Nacional de Educacion a Distancia,
[2]Univeridad de Extremadura and [3]Universidad de Castilla-LaMancha
Spain

1. Introduction

The *recognition* problem tries to identify an object, called unknown or *scene* object, from a set of objects in an object database, generally called *models*. The problem of *positioning* or *alignment* solves the localization of an object in a scene with respect to a reference system linked to the model of this object. One of the most common ways of solving this problem is *matching* the unknown object on the corresponding object in the object database. Although conceptually recognition and positioning are two different problems, in practice, especially when only part of the object is available (i.e. partial view), they are closely related. If we can align the unknown object precisely on one of the different objects in the database, we will have solved not only positioning but also recognition.

In a general sense, an object recognition system finds objects in the real world from an image of the world, using object models which are known a priori. There is a wide variety of approaches that propose different solutions to recognize 3D objects. Most of them use representation models based on geometrical features where the solution depends on the feature matching procedure. The method we present in this work is concerned with the case when only range data from a partial view of a given free-shaped object is available. Recognition must be carried out by matching this range data of the partial view with of all the possible views of every complete object in the stored object database. The resolution of the problem is of real practical interest since it can be used in tasks with industrial robots, mobile robot navigation, visual inspection, etc.

Regarding the kind of models used in the different approaches there are two fundamental 3D representation categories: object-based representation and view-centred representation. The first tries to generate the model according to the appearance of the object from different points of view, while the second creates models based on representative characteristics of the objects. More detailed information on them will be included in next section.

The structure of this chapter is as follows. Section 2 shows a short survey of recent and more important works that could be considered closer to our work. Section 3 is devoted to make a general description of the stages in which the proposed method is decomposed. The first stage and the WCC feature, which is the key of our method, are studied in detail in section

4. Some explanations of the two remaining stages are stated in section 5. Then, the main experimental results of the method are analyzed in section 6, making special emphasis in the high reduction rates achieved in the first stage. Section 7 states the conclusions of this work.

2. State of the art in 3D recognition methods

As it has been stated in the introduction, 3D recognition methods are highly dependent on the type of chosen representation to model the considered objects. Anyway, all the existing representation approaches belong to one of the two mentioned categories: view-centred representation and object-based representation.

In view-centred representations each object is described in terms of several intensity images taken from different points of view. They try to generate the object model according to the appearance of the object from diverse viewing directions. Representation techniques using aspect graphs or others using silhouettes, and mainly those methods based on principal components, belong to this category. Examples of the last one can be found in (Campbell & Flynn, 1999) of in (Skocaj & Leonardis, 2001).

Another view-based object recognition strategy is described in (Serratosa et al, 2003). They use a *Function-Described Graph (FDG)* that gives a compact representation of a set of attributed graphs corresponding to several views of polyhedral objects. Then the recognition process can be accomplished by comparison between each model and the graph of the unclassified object.

In the work of (Cyr & Kimia, 2004) the similarity between two views of the 3D object is quantified by a metric that measures the distance between their corresponding 2D projected shapes. A slightly different approach is proposed by (Liu et al., 2003), where the so called *Directional Histogram Model* is defined and evaluated for those objects that have been completely reconstructed.

Object-based representations try to model the object surface or the object volume by using significant geometric features referred to a local coordinate system. Representations in this category can be included in four major groups: curves and contours, axial, volumetric and surface representations respectively. The method proposed in this work can be included in the last group and, consequently, a more detailed analysis of the related techniques in this group is exposed next.

(Chua & Jarvis, 1997) code surroundings information at a point of the surface through a feature called *Point Signature.* Point signature encodes information on a 3D contour of a point P of the surface. The contour is obtained by intersecting the surface of the object with a sphere cantered on P. The information extracted consists on distances of the contour to a reference plane fixed to it. So, a parametric curve is computed for every P and it is called point signature. An index table, where each bin contains the list of indexes whose minimum and maximum point signature values are common, is used for making correspondences.

(Johnson & Hebert, 1999) have been working with polygonal and regular meshes to compare two objects through *Spin Image* concept. Spin image representation encodes information not for a contour but for a region around a point P. Two geometrical values (α, β) are defined for the points of a region and a 2D histogram, with α and β as coordinates, is finally constructed.

In (Yamani & Farag, 2002) a representation that stores surface curvature information from certain points produces images, called *Surface Signatures*, at these points. As a result of that, a standard Euclidean distance to match objects is presented. Surface signature

representation has several common points with spin image. In this case, surface curvature information is extracted to produce 2D images called surface signature where 2D coordinates correspond to other geometrical parameters related to local curvature.

The two last mentioned methods are halfway between the two basic categories since they do not capture the appearance of the object from each point of view, but provide just a characteristic measurement of the object. This is also our case since our basis will be different measurements on the meshes or on the range data of the objects, calculated from different points of view. In this particular direction is addressed the problem in (Adan & Adan, 2004) where a shape similarity measure is introduced and applied. Nevertheless, this solution does not solve satisfactorily the object recognition problem from real partial views, which is the main purpose of our method.

3. Overall method: Functioning principle

The method presented in this work obtains effective database reduction by applying sequentially different global characteristics calculated on the spherical meshes and the range data of partial views (Fig. 1).
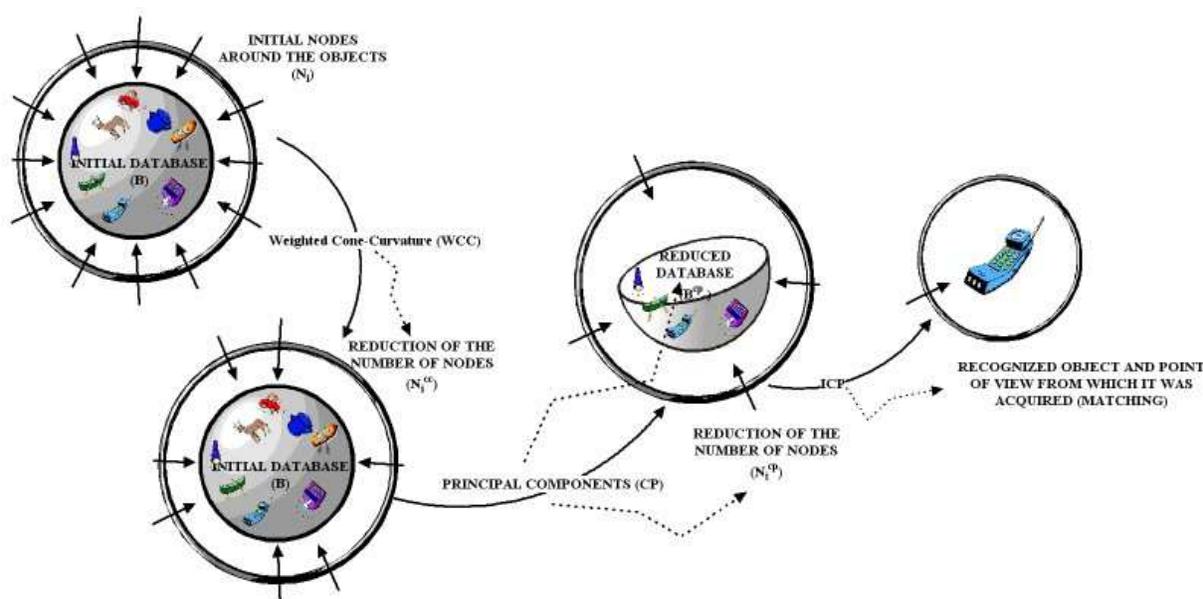

Fig. 1. Scheme of the different stages of the method for object recognition from partial views: graphical representation.

In the first stage we use a new invariant that we call *Weighted Cone-Curvature (WCC)* to determine a first approximation to the possible axes of vision from which this partial view has been acquired. Discretization of the vision space is obtained by circumscribing a spherical mesh around the model of the complete object. Each node in this mesh, together with the origin of coordinates, defines the initial axes of vision around this model. Therefore, determining the possible axes of vision from which the partial view has been acquired is equivalent to selecting a set of nodes on the mesh and rejecting the others. It is important to bear in mind that with this reduction what we are doing implicitly is a reduction of the possible rotations that could be applied on the partial view to match it on the model of the complete object.

We will call the nodes obtained after this first step $\mathbf{N}_i^{cc} \subset \mathbf{N}_i$, where $\mathbf{N}_i$ are the initial nodes of the spherical mesh circumscribed in the *i*-th object of the database. As is deduced from the explanation, in this stage the number of models in the object database is not reduced.

Another invariant based on the principal components (eigen values + eigen vectors) of the partial view and complete object range data will be applied in a second stage on the selected nodes. After this features comparison a list for each of the objects in the database will be created with the $\mathbf{N}_i^{cc}$ nodes ordered according to the error existing in the eigen values comparison. This ordering in turn means that it is possible to identify which object has the greatest probability of matching the partial view. At the end of this second stage a reduction of the models in the object database is obtained together with the reduction of the nodes determined in the previous stage. If we call the initial object database **B**, the base obtained after comparing the eigen values will be $\mathbf{B}^{pc} \subset \mathbf{B}$, and the nodes for each object $\mathbf{N}_i^{pc} \subset \mathbf{N}_i^{cc}$.

The eigen vectors will allow a first approximation to be done to the rotation existing between the partial view and each one of the objects of $\mathbf{B}^{pc}$, which will be used in the last stage when the *Iterative Closest Point (ICP)* algorithm (Besl and Mckay, 1992) is applied. This allows the matching to be done between the range data, and the convergence error of the algorithm will indicate the object to which the partial view belongs.

The last two stages of the method are based on conventional techniques, whereas the first one represents a novel way of dealing with this problem. Therefore, only this key stage of the applied method will be explained with more detail in next section.

4. First stage: Robust determination of the point of view

This is the most important phase of our approach because of its novelty. As it has been mentioned, the purpose of this stage in the overall recognition method is the estimation of the possible points of view from which the given partial view of the object has been acquired are estimated. For this task the new characteristic WCC, which is computed from the partial spherical model, is proposed. The specific partial modelling technique applied is not going to be explained in detail here, and a deeper analysis can be found in (Salamanca et al., 2000). Nevertheless, some preliminary concepts must be introduced to present and explain the power of this feature. First of all it must be said that the WCC feature is derived from the previous concept of *Cone-Curvature (CC)* defined in (Adan & Adan, 2004). But CC concept was originally introduced to represent complete models of objects and it is not directly applicable to partial modeling. Therefore, before establishing a WCC definition it is necessary to introduce the CC concept, and previous to it some spherical modeling basics should be expressed.

CC concept is an invariant feature defined on *Modeling Wave Models (MWM)* (Adan et al., 2000). These MWM were originally defined to represent complete models of objects. The surface representation of a complete object is defined over a mesh T_I of *h* nodes, being $h=ord(T_I)$, with 3-connectivity relationship derived from the tessellation of the unit sphere. Then T_I is deformed in a controlled manner until it fits the available range data of the complete object surface. This new mesh adjusted to the object surface is called T_M. It has exactly the same number *h* of nodes of the original tessellated sphere and is composed of hexagonal or pentagonal patches. Then, several geometric features can be extracted from T_M and mapped into T_I. In this way, models for all considered objects have the same number of nodes and equal mesh topology.

Let us call generically *T* to any of these meshes coming from the standard tessellated unit sphere. To make easier the features mapping and the subsequent searching algorithms, some others topological substructures can be defined around the standard mesh *T*. For example, any node *N* of the total *h* can be considered as *Initial Focus* of a new topological structure call *Modeling Wave Set (MWS)*. This MWS is built from another simpler structure called *Modeling Wave (MW)*. And the last one is composed by a collection of samples of other simpler structure called *Wave Front* (denoted as *F*).

In practical, given any initial focus *N*, its associated MW structure organizes the rest of the nodes of the mesh in disjointed subsets following a new relationship. Each subset contains a group of nodes spatially disposed over the sphere as a closed quasi-circle, resulting in subsets that look like concentric rings on the sphere. Since this organization resembles the shape of a wave, the name of Modeling Wave has been chosen to call it. With similar reasoning, each of the disjointed ring-shaped subsets is known as Wave Front, and initial node *N* is called Focus. Of course, the MW structure remains in *T* across the deformation and fitting process, as it can be seen in Fig. 2.

From the previous ideas it can be deduced that any node of *T* may be focus and can generate its own MW. Therefore *h* different MWs can be generated in a model, being the set formed by these *h* MWs what constitutes the Modeling Wave Set.
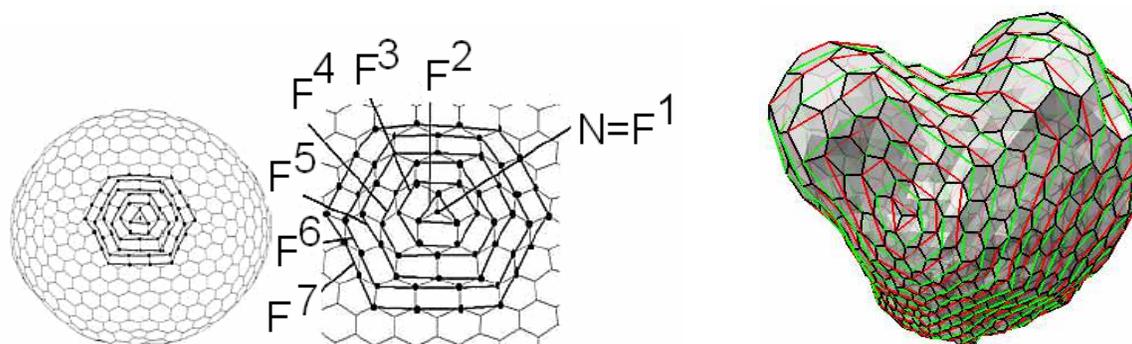

Fig. 2. Left, the first seven consecutive WFs drawn over the standard unit sphere T_I. Right, fitted T_M mesh (corresponding to a complete object) with several WFs plotted on it.

These substructures can be formally defined as follows:

Definition 1. Let N be any node of the tessellated sphere T, and let us call it Initial Focus. Let F^j be the j-th Wave Front associated to the Initial Focus N, with j = 1 ... q-1. The consecutive Wave Fronts verify the following construction law:

$$F^1 = \{N\} \tag{1}$$

$$\vdots$$

$$F^{j+1} = V(F^j) - \bigcup_{m=1}^{j-1} F^m \quad \forall j = 1, \cdots, q-1 \tag{2}$$

where V represents the three-neighbour local relationship imposed by T.

Definition 2. *Let MW^N be the Modeling Wave with Initial focus N. MW^N is a partition of the tessellated sphere T integrated by the q consecutive Wave Fronts associated to the Initial Focus N, i.e., $MW^N = \{F^1, F^2, \ldots, F^q\}$.*

It is important to notice that each node of the standard mesh together with its origin of coordinates configures a different viewing direction. Therefore, each viewing direction has associated a Modeling Wave. Fig. 3 shows two MWs on the tessellated sphere and the axes of vision defined by the focus and the origin of coordinates in both cases.
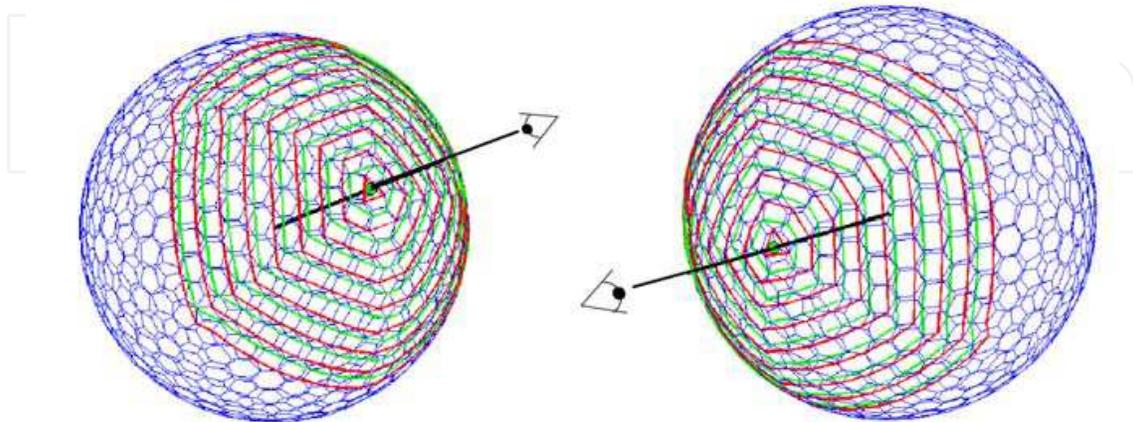

Fig. 3. Representation of two Modeling Waves on the tessellated sphere. Each MW is associated to a different point of view

Definition 3. *We call Modeling Wave Set associated to T to the integration of all the Modeling Waves that can be built from the nodes of T, i.e., MWS = {MW^1, MW^2, ... , MW^h}, where MW^i, i = 1 ... h, is the Modeling Wave with the i-th node of T as Initial Focus.*

In order to adapt the MWS representation to partial data we have developed a partial MWS modeling procedure. Two half-spheres can be defined along the viewing direction; one in front, called $T_{1/2}$, and the other one at the back. The process is based on deforming the first one half-sphere $T_{1/2}$, while the second one is rejected. An approximation stage of $T_{1/2}$ to the normalized object data points and a posterior local regularization stage are performed in order to get the deformed mesh to be as uniform as possible. The result is a set of nodes, denoted generically as T' instead of T, fixed to the surface data as much as possible. Fig. 4 illustrates some aspects of this procedure, but a more detailed explanation can be found at (Salamanca et al., 2000).

Notice that now the number of nodes of each partial model is usually different to each other and it is less than the number of nodes in the standard unit sphere, i.e. $h' = ord(T') \neq h$. Contrary to complete model, the Modeling Wave structure appears broken in the partial models. Consequently when part of the surface of an object is available we just adapt the method taking the set of complete Wave Fronts that appears in the partial model corresponding to the partial view. In fact, spherical features of an object must now be calculated from its partial spherical model T', which has been created from the range data of a given partial view. After the mentioned mesh adjustment process, the obtained T' mesh also has hexagonal or pentagonal patches. Each of the nodes of this mesh has a connectivity of 3 except for those nodes that are in the contour with connectivity less than 3. Fig. 5 shows the intensity image of an object and the obtained spherical model for a partial view of the object acquired from a given point of view. Partial mesh has now much less nodes than the standard unit sphere. Contour nodes are drawn in red in the right half of Fig.5.
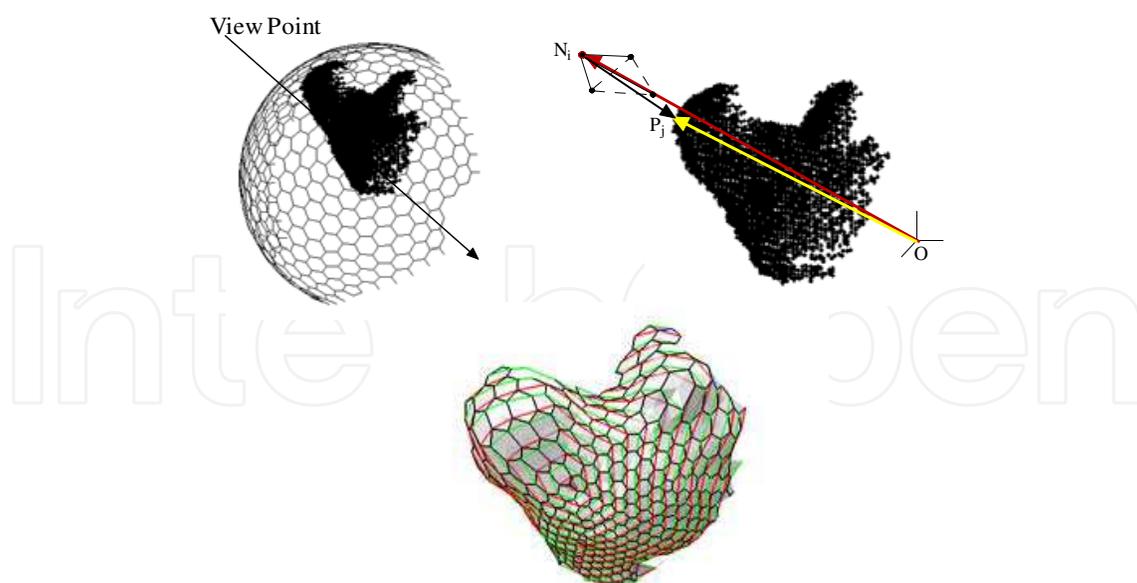
Fig. 4. Partial view modeling. Left above, $T_{1/2}$ associated to normalized object data points. Right above, approximation process. Bellow, partial model showing some broken WFs
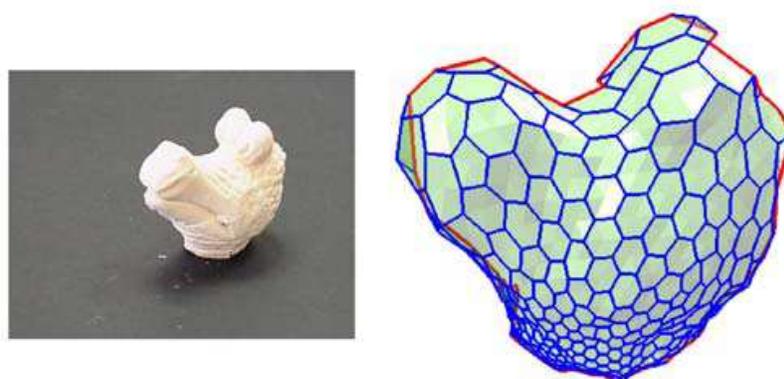

Fig. 5. Intensity image of an object and spherical model for a partial view of the object.

4.1 Cone-Curvature. Concept, definitions and properties

Once the modeling structure has been created is time to compute discrete values of some three-dimensional object features and storing them conveniently in the MWS structure. So, it is possible to map global and local features of T_M over T_I considering 3-connectivity, like discrete curvature measurements (Hebert et al., 1995), colour features, distance to the origin of coordinates, etc. In this case, Cone-Curvature (CC) represents an intuitive feature based on the MW structure taking into account the location of the WFs inside the model T_M. In the following formal definition of CC we will use generically T' to call to the spherical mesh because this definition is applicable both to complete and partial meshes.

Definition 4. *Let N be Initial Focus on T'. We call j-th Cone Curvature α^j of N to the angle of the cone with vertex N whose surface is fitted to the j-th Wave Front of the Modeling Wave associated to N. Formally:*

$$\alpha^j = sign(F^j) * \left| \frac{\pi}{2} - \frac{1}{t_j} \sum_{i=1}^{t_j} \gamma_i^j \right| \tag{3}$$

$$\gamma^j_i = \angle C^j N N_i \ , \ N_i \in F^j$$

where t_j is the number of nodes of F^j and C^j is the barycentre of F^j. The range of CC values is $[-\pi/2, \pi/2]$, being the sign assigned taking into account the relative location of O, C^j, and N, where O is the origin of the coordinate system fixed to T' (see Fig. 6).

Given a focus N, there exists a set of wave fronts, q, which define the CCs for this focus $\{\alpha^1, \alpha^2, \alpha^3, \dots \alpha^q\}$ that provide complete information about the curvature of the surroundings of N. Finally, q, which we call *Front Order*, can have values from 2 (case $q = 1$ does not make sense) to the maximum number of fronts that the object has. As we want to work with partial models, the maximum order corresponds to the higher complete Wave Front.
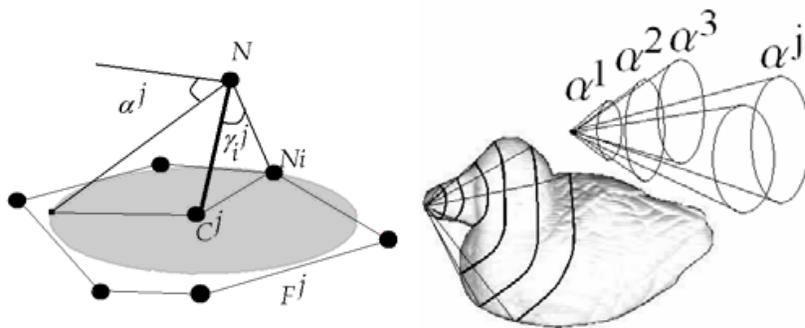

Fig. 6. Left, definition of the CC. Right, visualization of the CC for a node N

Next we will analyze several meaningful properties of CC on MWS models. These properties can be summarized as: uniqueness, invariance to affine transformations (translation, rotation and scaling), robustness and adaptability.

Fig. 7 plots a set of CCs $\{\alpha^1, \alpha^2, \alpha^3, \dots \alpha^q\}$ $q = 18$, for different nodes of a mesh model. In this case the locations of the nodes correspond to different areas in the mesh. Note that their CC
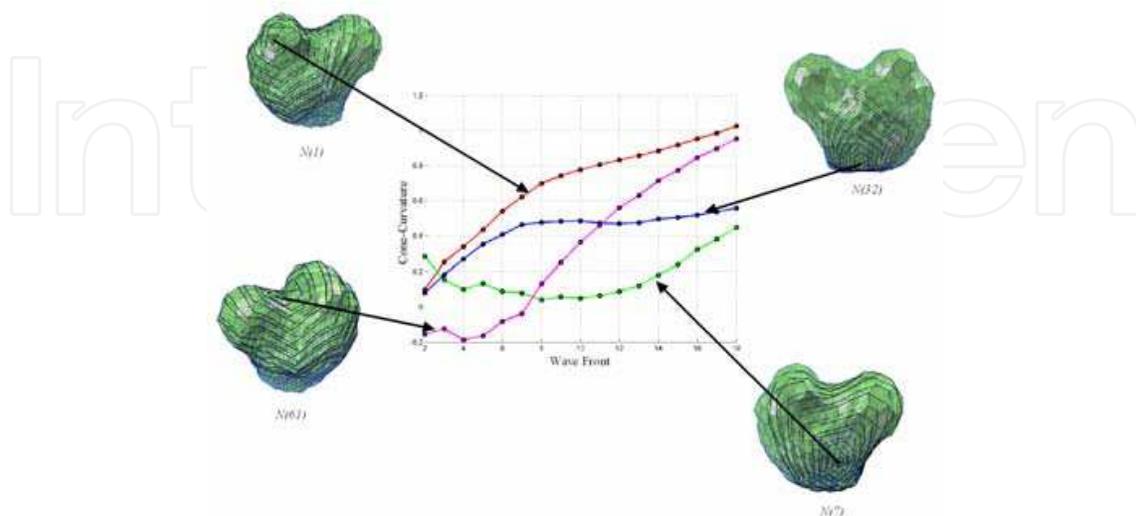

Fig. 7. Representation of CC ($\{\alpha^1, \alpha^2, \alpha^3, \dots \alpha^q\}$, $q = 18$), for the nodes $N(1)$, $N(7)$, $N(32)$ and $N(61)$ of T_M.

distributions are very distant. Consequently different zones of an object can be represented and recognized by a CC vector.

In Fig. 8 the mesh T' has been coloured to represent the values of the CCs for different orders (2, 8, 14 and 16). As it can be seen, there exists continuity in the colours of the mesh in both cases: for the same order (i.e. between the nodes of a same mesh) and for different orders (i.e. between the nodes of the different meshes). On the other hand, the change in colour (equivalent to the change in the CC) is much less in the lower orders. This means that high orders give poorer information than lower orders.

In order to demonstrate that CC is invariant to affine transformations Fig. 9 shows the CCs after carrying out a set of random rotations, translations and scaling. Models and CC graphs for five cases can be seen in it. Note that CC vectors suffer a little variation in all cases.
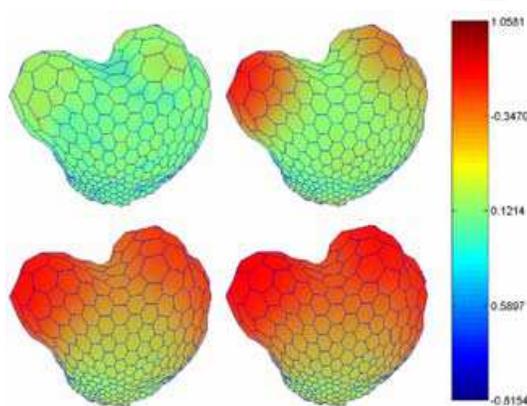

Fig. 8. Representation in colour of the cone-curvatures in each mesh node for orders 2, 8, 14 and 16 (left to right and from top to bottom). A bar is also shown where the colours for the maximum, mean and minimum cone-curvatures of the object can be seen.
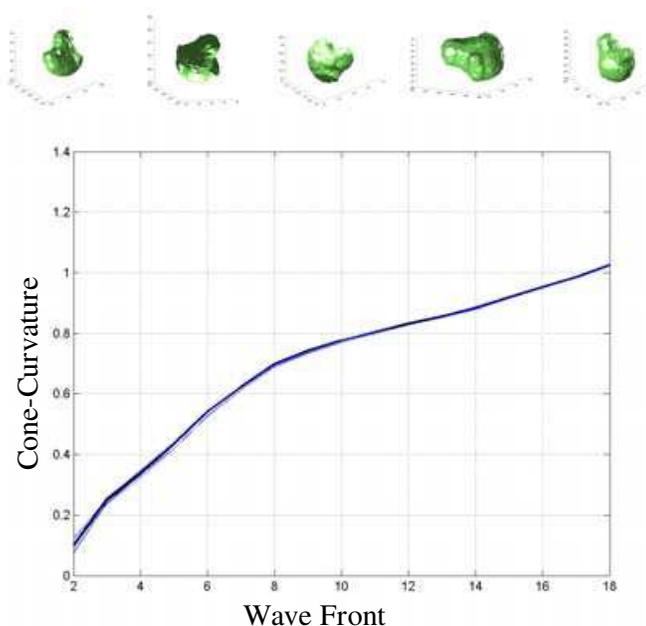

Fig. 9. CCs for five free-form models obtained from rotation, translation and scaling of the original range data. The invariance existing in this measurement can be seen.

Next property is concerning to the robustness of the CCs. In this case, a random noise has been generated for each node proportional to the inter-node mean distance. Fig. 10 shows the meshes and cone-curvatures for 0%, 5%, 10%, 25%, 50% and 100% of noise. The colour used for drawing the meshes is the same colour as in the graphs of the CCs. In all these graphs it can be seen that CCs remains invariant for normal noise levels.
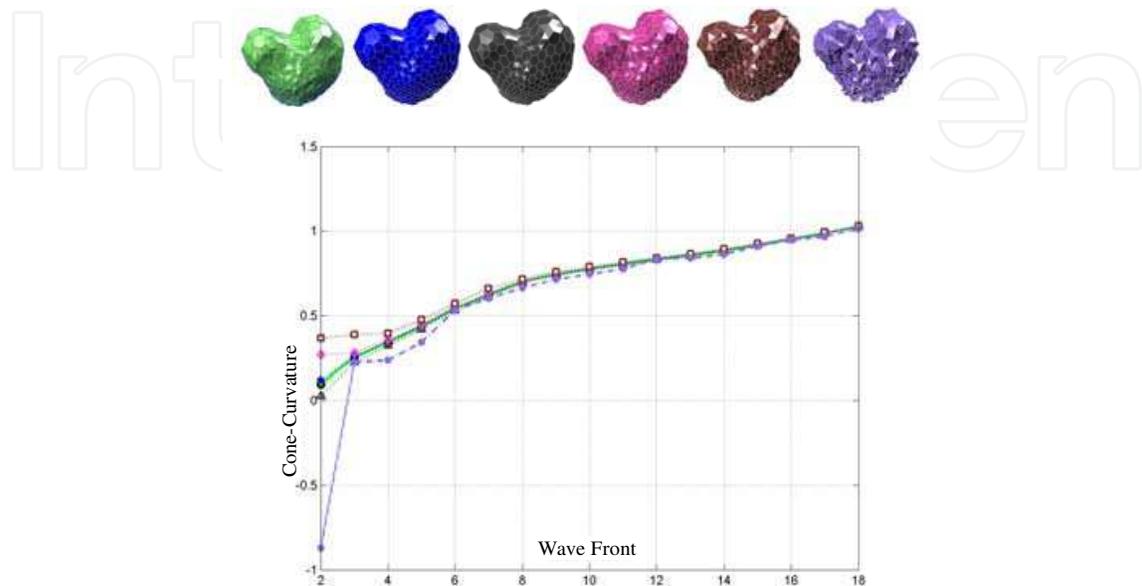

Fig. 10. Representation of CCs with different levels of noise in the mesh (0%, 5%, 10%, 25%, 50% y 100%). The colour used of the meshes is the same as in the representation of CC.

Finally CC concept is flexible or adaptable in the next sense. As it has been said in previous paragraphs the CC values depend on the depth level over the MW structure. So, different combinations with respect to different criteria could be chosen for exploring an object (model) through its CC. For instance, we can consider a wide range of criteria: explorations for only one WF for low levels, for medium levels and for high levels. On the other hand we can choose explorations using contiguous/discontiguous Wave Fronts throughout the whole MW structure. This means that, using the object model and following different criteria, a wide variety of parts of the object (or depth levels) can be chosen in order to recognize an object. This property is obviously the key for performing further recognition approaches in partial and occluded scenes as will be discussed in the next section.

4.2 Weighted Cone-Curvature (WCC)

In order to apply the CCs to the recognition of partial views several factors have to be considered in advance:

1. The number of complete wave fronts in a partial view is variable.
2. The number of wave fronts can vary between a partial model and its corresponding complete model.
3. The mean length of the internode distance is different for the partial model and the complete model in the same object.

These questions imply that one-to-one comparison between the CCs of the same order between the partial and total models could be inefficient. Therefore, we have used a more

compact information from the CCs which reduces the dimensionality, replacing each CC vector $\{\alpha^1, \alpha^2, \alpha^3, ...\alpha^q\}$ with a scalar that summarizes the information of q CCs. Thus each node of a model has a single value associate and, consequently, an object is characterized by h values, h being the number of nodes of the corresponding model. We call this feature Weighted Cone-Curvature (WCC).

To evaluate quantitatively if the proposed reduction is possible, the correlation existing between the CCs was calculated. This is shown in gray scale in Fig. 11 (white for high values and black for low values), and it has been calculated as the mean value of all the correlation coefficients of the meshes in the database. From analysis of the figure, and as we had envisaged, it can be concluded that there is a high correlation between fronts of near orders, which increases as this order increases.
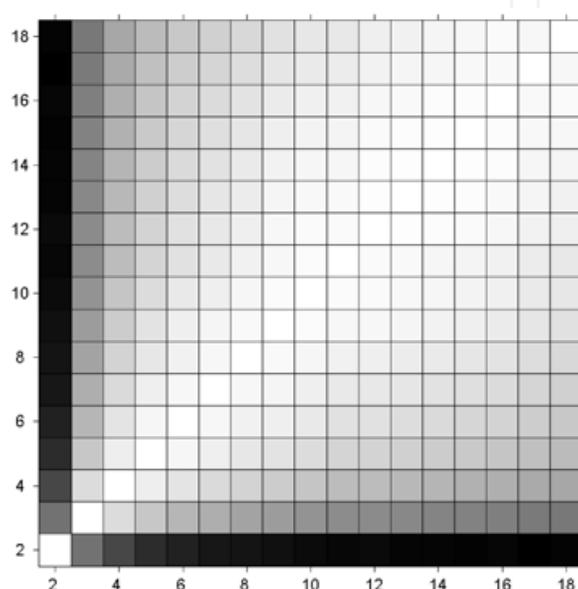

Fig. 11. Illustration of the correlation existing between the Cone-Curvatures of the wave fronts of orders 2 to 18 in the database.

If we denote the WCC for each $N' \in T'$ as c^w, the linear combination will be:

$$c^w = \sum_{j=1}^{q} v^j \alpha^j \qquad (4)$$

where v^j are the coordinates of the eigen vector associated with the eigen value of greater value of the covariance matrix for the q initial variables.

This eigen vector was determined empirically by evaluating the principal components on the Cone-Curvatures of all the mesh nodes. As regards the orders considered, we studied three possibilities:

1. Wave fronts from $q = 2$ to $q = 18$.
2. Wave fronts from $q = 4$ to $q = 18$.
3. Wave fronts from $q = 4$ to $q = 9$.

Fig. 12 represents, for the object that we are analyzing, the WCCs in the three cases, plotted over the object mesh and using a colour code to express the range from negative to positive values. We can see that the WCCs for the first and second cases are very similar.
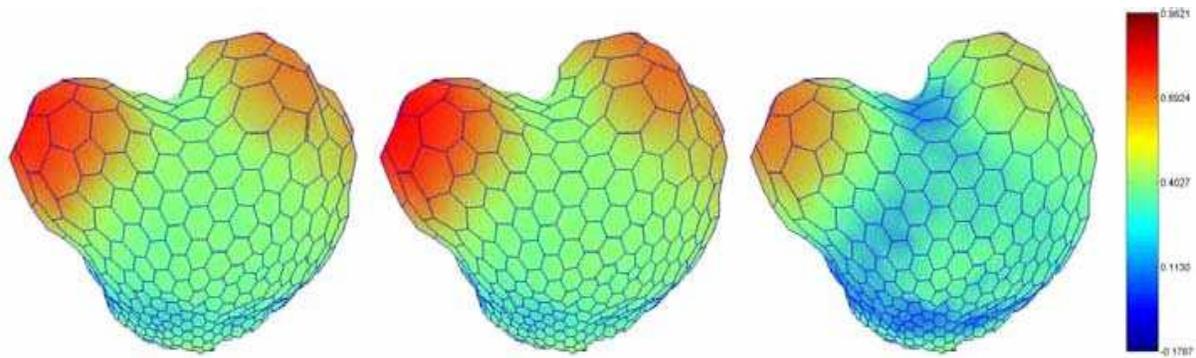
Fig. 12. Representation in colour of the WCCs of each mesh node for cases (1), (2) and (3) (left to right). A bar is shown where the colours can be seen for the maximum, mean and minimum WCCs of the object.

4.3 Application of WCC to partial views recognition

WCCs allow us to carry out a selection of regions on a complete object model that can be similar to a specific region of the scene. For this selection, an error measurement between scene and model is defined as follows:

Definition 5. *Let $N' \in T'$ be the node of the partial mesh T' which is the nearest to the axis of vision. The error or distance of comparison of weighted cone-curvatures for each $N \in T_i$, where T_i is the i-th total model of the object database is defined as:*

$$e_j(N) = \left| c^{w'}(N') - c^w(N_j) \right|$$ (5)

where the subscript j extends from 1 to the maximum number of nodes existing in T_i and $|\bullet|$ represents the absolute value.

The fact of conditioning the reduction of nodes around T_i to just one measurement of error can cause significant errors in this reduction. Therefore, in order to reinforce the reduction, for each $N \in T_i$ two errors will be measured. The first will consider the WCC's to the furthest fronts generated from N'. We will call this error deep error and give it the symbol $e_j^p(N)$. The second will consider the nearest fronts generated from N'. This time we will call the error superficial error and give it the symbol $e_j^s(N)$.

In both instances a set of errors equal to the number of nodes existing in T_i is obtained, and from these errors the nodes $\mathbf{N}_i^{cc}$ of the mesh that will be passed to the next stage of the algorithm will be determined. If we call $\mathbf{N}^p$ to the set of nodes of T_i with less e_i^p values, and $\mathbf{N}^s$ to the set of nodes of T_i with less e_i^s values, $\mathbf{N}_i^{cc}$ will be:

$$\mathbf{N}_i^{cc} = \mathbf{N}^p \cup \mathbf{N}^s$$ (6)

5. Principal components and ICP stages

In this section the last two stages of the recognition algorithm will be commented on for matching the partial views on complete models. These are the principal components and ICP stages. In the principal components stage the method proposed is based on calculating the principal components on the range data that we employed to obtain the model T' used

in the previous stage. If we call these data **X**, the principal components are defined as the eigen values and eigen vectors $\{(\lambda_i, \vec{e}_i) \quad i = 1, \cdots, m\}$ of the covariance matrix.

The eigen values are invariant to rotations and displacements and the eigen vectors to displacements. The eigen vectors conform a reference system linked to the data. This means that the eigen values can be used to evaluate what part of the range data of the complete model correspond to the scene, and the eigen vectors to calculate a first approximation to the transformation of the partial data to be matched on the total data. This approximation will only reflect the rotation sub matrix of the total transformation, since the origins of the two frames will coincide.

To apply this technique it is necessary to evaluate, before the recognition process, all the possibly existing partial views on the range data of the complete object. For this, the space of the possible points of view existing around the object was discretized, and a method was developed for generating *virtual partial views (VPV)* based on the z-buffer algorithm. From each of these VPV their principal components will be calculated and used in the matching stage as explained earlier.

Comparison of the eigen values gives information about the possible areas where the partial view can be matched, but this information is global and, as we have said, only gives information about the rotation.

Thus it will be necessary to do a final calculation stage to refine the matching and to calculate the definitive transformation. For this we will use the ICP algorithm on a number of possible candidates marked in the eigen value comparison stage. The ICP must start from an approximation to the initial transformation, which in our case corresponds to the transformation given in the matching of the eigen vectors. The ending error in the ICP algorithm will measure the exactness of the definitive transformation and the correctness of the area where the view will be matched.

The comparison of the eigen values of the partial view and the virtual partial views is done by measuring an index of error given in the following expression:

$$e_i^{pc}(N) = \left\| \Lambda_i^v(N) - \Lambda^r \right\| \tag{7}$$

where $N \in \mathrm{N}_i^{cc}$ is the node from where we generated the VPV, $\Lambda_i^v(N)$ is the vector formed by the eigen values of the VPV generated from the node *N* of the i-th object of the object database (*i=1,..., K*), $\Lambda^r = \{\lambda_1^r, \lambda_2^r, \lambda_3^r\}$ is the vector formed by the eigen values of the real partial view and $\| \bullet \|$ is the Euclidean distance.

After the error has been calculated for all the $\mathbf{N}_i^{cc}$ nodes and all the objects in the object database, we obtain a list of these errors, e_i^{pc} (*i=1,..., K*), ordered from least to great. If we compare the first error (least error for a set object) in all the lists, an ordering of the different objects in the object database will be obtained. Thus in the last stage we can apply the ICP algorithm on a subset of the object database, just $\mathbf{B}^{pc}$, and for each of the objects using the transformations associated with the subset of nodes that have produced these errors.

For the resolution of the ICP it is necessary to determine an approximation to the transformation matrix R_1, between the partial view and the object in the object database. It is determined by applying the Horn method (Horn, 1988). This is calculated bearing in mind that the eigen vectors are orthonormal, and therefore:

$$R_1 = E^r(E_i^v(N))^{-1} = E^r(E_i^v(N))^T \qquad (8)$$

where $E_i^v(N)$ are the eigen vectors of the VPV generated from $N \in \mathbf{N}^{pc}$ of the i-th model of the object database $\mathbf{B}^{pc}$, and E^r are the eigen vectors of the partial view.

6. Experimental results

The method presented in this work has been tested over a set of 20 objects. Range data of these objects have been acquired by means of a range sensor which provides an average resolution of approximately 1 mm. Real size of the used objects goes from 5 to 10 cm. height and there are both polyhedral shaped and free form objects (see Fig. 13). MWS models have been built by deforming a tessellated sphere with *h*=1280 nodes.

Fig. 13. Image of the objects used in the test of the algorithm.

The recognition was done for three partial views per object, except in one of them where after the determination of its partial model it was seen that it did not have enough wave fronts to be able to compare the weighted cone-curvatures. This means that recognition was done on a total of 59 partial models. The success rate has been the 90%, what demonstrates the validity of the method. The average computation time invested by the whole process was 90 seconds, programmed over a Pentium 4 at 2.4 GHz. computer under Matlab environment. A more detailed analysis of these results is next.

As it has been explained, in the first stage the weighted cone-curvatures of the partial model were compared for a node with a maximum number of wave fronts. From this comparison $\mathbf{N}_i^{cc}$ was determined (equation (6)). In the considered experiments, the maximum value of the number of nodes that form the sets $\mathbf{N}^p$ (deep search) and $\mathbf{N}^s$ (superficial search) was 32 each. Since the mesh used to obtain the complete model T_i was 1280, the minimum reduction of the space search in this stage was 95%. The reduction can be even bigger as long as there are nodes coinciding in $\mathbf{N}^p$ and $\mathbf{N}^s$. This step was carried out for all the objects of the initial database $\mathbf{B}$ and took an average of 7.95 seconds.

Concerning the second stage, it started from these nodes and the eigen values were compared, which allowed us to achieve the first reduction of the database ($\mathbf{B}^{pc}$ database). Reduction of the nodes obtained in the previous stage is also accomplished ($\mathbf{N}_i^{pc}$ set). It was determined experimentally that $\mathbf{B}^{pc}$ consists of approximately 35% of the objects of $\mathbf{B}$ and $\mathbf{N}_i^{pc}$ of approximately 8% of the nodes of $\mathbf{N}^{cc}$ per object, which represent very satisfactory reduction rates of the stage. This process spent around 1 sec.

Finally, the ICP algorithm was applied on seven objects (the mentioned 35% remaining in the $\mathbf{B}^{pc}$ database) and three nodes (corresponding to the mentioned 8%) for each $\mathbf{N}_i^{pc}$ object. As it can be deduced, most of the time invested by the algorithm was practically consumed in this stage.
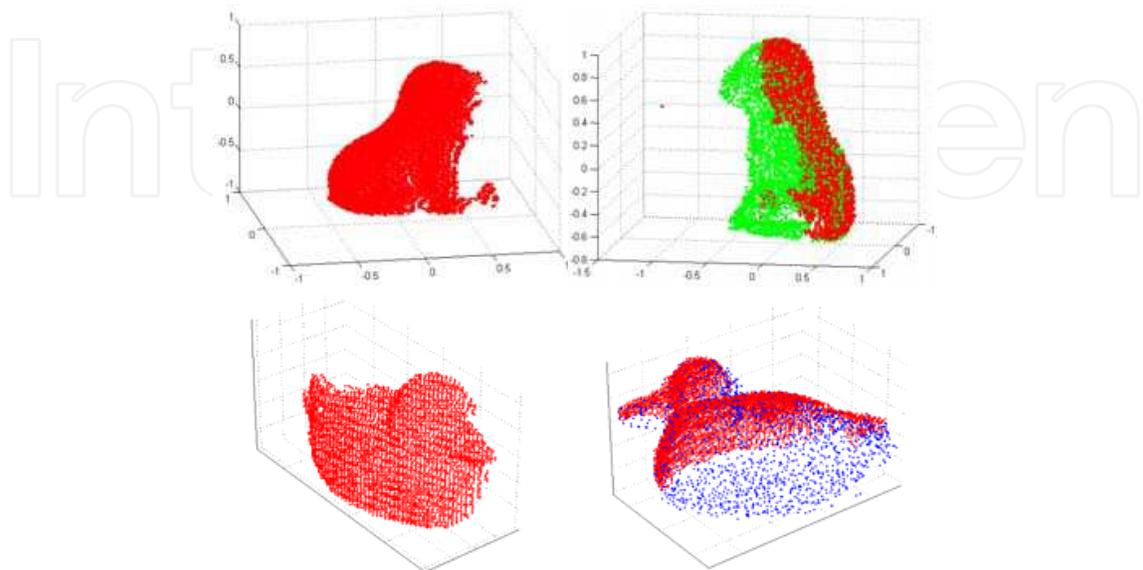

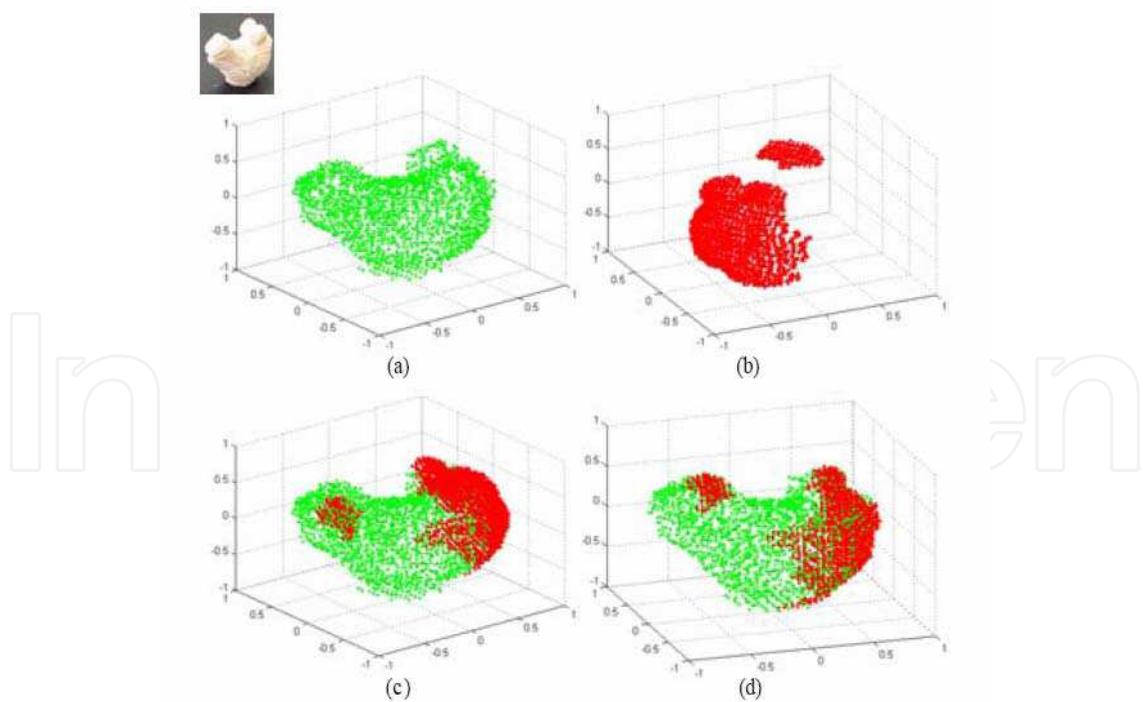Fig. 14. Results obtained with several scenes of free-form objects without auto-occlusion

Fig. 15. Details of the process in a case of auto-occlusion. In (a) we can see the range data of the complete object, in (b) the range data of the scene which we want to recognize, and the result before (c) and after (d) ICP application.

Fig. 14 shows the results obtained with several scenes consisting of free-form objects. In these examples scene range data is superimposed to the complete object. Fig. 15 illustrates details of this process in a case of auto-occlusion. Part (a) presents the range data of the complete object, part (b) corresponds to range data of the scene, part (c) shows both range data superimposed after the raw transformation obtained in the principal components stage is applied and part (d) contains the final results after ICP algorithm application. Some plots have been rotated to enhance data visualization.

Complementary tests of this recognition procedure have been carried out in slightly different environments, for example in (Salamanca et al., 2007). Nevertheless, no significant performance differences can be extracted from the analysis of the obtained results in all these cases.

7. Conclusions

This work has described the experiences with a method for the recognition of free-form objects from their partial views. The method is divided into three stages: Weighted Cone-Curvatures stage, Principal Components stage, and ICP stage, being the first one the most effective from the recognition point of view. Due to this fact and to the originality of the handled features, this stage has been described in more detail in the chapter.

A new feature called Weighted Cone-Curvature is used in the first stage. This feature is measured on the spherical model built from the object range data. Its definition and application have been extended from the originally designed case of complete objects to the more specific case when only partial viewing of the objects are available. By the way, and as it has been stated, this has been the main objective of the present work. The basics of spherical modeling have been included, as well as the method for computing the WCC in complete and partial objects models. From the analysis of the WCC feature it has been demonstrated that it exhibits very adequate properties for applying in recognition and positioning tasks. These characteristics allow achieving important reductions in the number of nodes that define the possible axes of vision from which the partial view has been acquired. In fact, the experiments presented in this work have shown that the reduction rate is, as minimum, of 95%, what means in practice a very significant reduction.

In the last two stages of the algorithm the definitive candidate is searched looking for the best matching of the partial view with the candidates of the previous stages. In the first of these two stages, the eigen values of the Principal Components of the partial view are compared with those Principal Components virtually extracted from the complete models just in the directions determined in the WCCs stage. By means of this stage we reduce again the nodes that define the possible axes of vision and the original database. We also calculate, from the eigen vectors of the Principal Components, a first approximation to the transformation matrix between the partial view and the complete object. Finally, in the second of these two stages, the ICP algorithm is applied and the selected candidate is chosen as a function of the convergence error. The fine transformation matrix is also estimated at this point.

The validity of the full method was proven with the recognition of 59 partial views in an object database of 20 objects, both polyhedral and free-shaped. The global success rate was 90%.

In contrast, two minor limitations of the algorithm can be mentioned. In first place, the use of spherical models restricts the applicability of the method since it does not allow coping with objects with genus different to zero. Even more, the spherical modeling technique by

itself is extremely complex. On the second hand, the time of execution of the algorithm is high, which means that its application in real time systems is not possible. At this concern it must be said that the algorithm it has been completely programmed in Matlab, what means a significant slowing down in execution time. Nevertheless, all the algorithms using representations like ours that have been mentioned in the introduction present this limitation.

8. Acknowledgements

9. References

Adan, A.; Cerrada, C. & Feliu, V. (2000). Modeling wave set: Definition and application of a new topological organization of 3D object modelling. *Computer Vision and Image Understanding*, Vol. 79, No. 2, (August 2000) 281–307, ISSN 1077-3142

Adan, A. & Adan, M. (2004). A flexible similarity measure for 3D shapes recognition. *IEEE Transactions on Pattern Analysis and Machine Intelligence*, Vol. 26, No. 11, (November 2004) 1507–1520, ISSN 0162-8828

Besl, P.J. & McKay, N.D. (1992). A method for registration of 3-D shapes. *IEEE Transactions on Pattern Analysis and Machine Intelligence*, Vol. 14, No. 2, (February 1992) 239–256, ISSN 0162-8828

Campbell, R.J. & Flynn, P. J. (1999). Eigenshapes for 3D object recognition in range data, *Proceedings of the IEEE Conference on Computer Vision and Pattern Recognition*, Vol. 2, pp. 2505–2510, Fort Collins, Colorado, USA, June 1999, IEEE Computer Society

Chua, C. S. & Jarvis, R. (1997). Point signatures: A new representation for 3D object recognition. *International Journal of Computer Vision*, Vol. 25, No. 1, (October 1997) 63–85, ISSN 0920-5691

Cyr, C.M. & Kimia, B.B. (2004). A similarity-based aspect-graph approach to 3D object recognition. *International Journal of Computer Vision*, Vol. 57, No. 1, (April 2004) 5–22, ISSN 0920-5691

Hebert, M.; Ikeuchi, K. & Delingette, H. (1995). A spherical representation for recognition of free-form surfaces. *IEEE Transactions on Pattern Analysis and Machine Intelligence*, Vol. 17, No. 7, (July 1995) 681–690, ISSN 0162-8828

Horn, Berthold K.P. (1988). Closed form solutions of absolute orientation using orthonormal matrices. *Journal of the Optical Society of America A*, Vol. 5, No. 7, (July 1988) 1127–1135, ISSN 1084-7529

Johnson, A.E. & Hebert, M. (1999). Using spin images for efficient object recognition in cluttered 3D scenes. *IEEE Transactions on Pattern Analysis and Machine Intelligence*, Vol. 21, No. 5, (May 1999) 433–449, ISSN 0162-8828

Liu, X; Sun, R.; Kang, S. B. & Shum, H.Y. (2003). Directional histogram for three-dimensional shape similarity, *Proceedings of the IEEE Conference on Computer Vision and Pattern Recognition*, Vol. I, pp. 813–820, Los Alamitos, California, USA, June 2003, IEEE Computer Society

Salamanca, S.; Cerrada, C. & Adan, A. (2000). HWM: a new spherical representation structure for modeling partial views of an object. *Proceedings of the International Conference on Pattern Recognition (ICPR'2000)*, Vol. 3, pp. 770–773, Barcelona, Spain, September 2000, IEEE Computer Society

Salamanca, S.; Adan, A., Cerrada, C., Adan, M.; Merchan, P. & Perez, E. (2007). Reconocimiento de objetos de forma libre a partir de datos de rango de una vista parcial usando cono curvaturas ponderadas. *Revista Iberoamericana de Automatica e Informatica Industrial*, Vol. 4, No. 1, (Enero 2007) 95–106, ISSN 1697-7912

Serratosa, F.; Alquezar, R. & Sanfeliu, A. (2003) Function-described graphs for modelling objects represented by sets of attributed graphs. *Pattern Recognition*, Vol. 36, No. 3, (March 2003) 781–798, ISSN 0031-3203

Skocaj, D. & Leonardis, A. (2001). Robust recognition and pose determination of 3-D objects using range image in eigenspace approach, *Proceedings of 3rd International Conference on 3D Digital Imaging and Modeling (3DIM 2001)*, pp. 171–178, Quebec City, Canada, May-June 2001, IEEE Computer Society

Yamany, S. & Farag, A. (2002). Surfacing signatures: An orientation independent free-form surface representation scheme for the purpose of objects registration and matching. *IEEE Transactions on Pattern Analysis and Machine Intelligence*, Vol. 24, No. 8, (August 2002) 1105–1120, ISSN 0162-8828
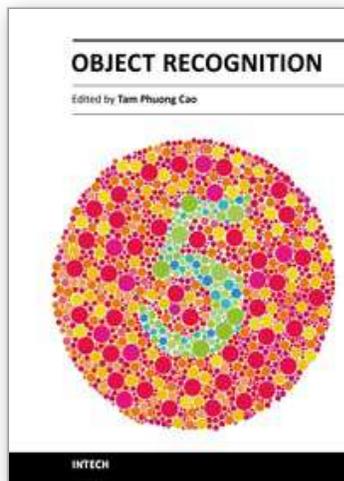
Object Recognition

Edited by Dr. Tam Phuong Cao

Vision-based object recognition tasks are very familiar in our everyday activities, such as driving our car in the correct lane. We do these tasks effortlessly in real-time. In the last decades, with the advancement of computer technology, researchers and application developers are trying to mimic the human's capability of visually recognising. Such capability will allow machine to free human from boring or dangerous jobs.

How to reference

In order to correctly reference this scholarly work, feel free to copy and paste the following:

INTECH
open science | open minds